Chinese Journal of Mechanical Engineering

ORIGINAL ARTICLE

Open Access

Prediction of Coefficient of Restitution for Impact Elastoplastic Spheres Considering Finite Plate Thickness

Yunfeng Fan[1], Hao Wang[2], Tao Zhou[1], Limin Zou[3,4], Zhinong Jiang[1,3] and Minghui Hu[1,3*]

Abstract

Collisions between objects are a relatively common phenomenon in nature. Analyses of collision processes can greatly contribute to solving problems such as impact-rub faults and particle impacts. The coefficient of restitution is a critical parameter in the analysis of collision processes. Many experiments have shown that the coefficient of restitution is closely related to the plate thickness, and the smaller the plate thickness, the more inaccurate the coefficient of restitution predicted by the existing model, which seriously affects the process of collision analysis. To remedy this shortcoming, this paper proposes a plate thickness influence factor with the ratio of sphere diameter to plate thickness as the variable. The plate thickness influence factor can optimize the coefficient of restitution model to effectively predict the coefficient of restitution of impacting elastoplastic spheres with finite plate thickness. Finally, the validity of the new model is verified using a large amount of experimental data.

Keywords Collision, Coefficient of restitution, Energy loss, Sphere

1 Introduction

Collisions are a common phenomenon in nature and are no exception in mechanical systems. When collisions occur, they can cause damage to productivity and even to the machine itself, such as rotor impact-rub faults [1–6]. To effectively minimize losses, it is important to analyse the collision process. The coefficient of restitution has received much attention as a parameter that can characterise the amount of energy lost during a collision without understanding the collision process in detail, but only by focusing on the object's motion before and after the collision. Ever since Newton [7] introduced the concept of the coefficient of restitution, there has been a controversy about the coefficient of restitution. Currently, there are three different ways to define the coefficient of restitution [8–11], but Newton's definition of the coefficient of restitution is still widely accepted and used [12]. In addition, the coefficient of restitution is often considered a constant determined by the material. However, studies have shown that the coefficient of restitution is influenced by factors such as the speed at the start of the collision and the yield strength. Yao et al. summarises the focus of controversy related to the collision coefficient of restitution, explains the three different definitions of the coefficient of restitution, and summarises the analysis of whether the three types of collision coefficient of restitution can be equated and the advantages and disadvantages based on the conclusions of previous studies by related scholars. In addition, the paper summarises the correlation between the coefficient of restitution and

*Correspondence:
Minghui Hu
humh2008@163.com
[1] State Key Laboratory of High-end Compressor and System Technology, Beijing University of Chemical Technology, Beijing 100029, China
[2] China Ship Research and Development Academy, Beijing 100101, China
[3] Key Lab of Engine Health Monitoring-Control and Networking of Ministry of Education, Beijing University of Chemical Technology, Beijing 100029, China
[4] Beijing Key Laboratory of High-End Mechanical Equipment Health Monitoring and Self-Recovery, Beijing University of Chemical Technology, Beijing 100029, China

other factors and their application in calculating collision dynamics [13].

In the existing literature, the analytical solution of the coefficient of restitution has been studied in detail by numerous scientists. In 1997, Thornton developed a simplified theoretical model of the interaction of two elastoplastic spheres in usual contact [14]. The model completely ignores the elastoplastic mixed phase and uses the yield stress as a boundary to distinguish between the elastic and plastic phases. Furthermore, the analytical solution of the coefficient of restitution was obtained by analysing the loading and unloading phases of elasticity and plasticity. Wu et al. [15] used the finite element method to study the collision of an elastic sphere with an elastic or elastoplastic substrate and obtained a coefficient of restitution model applicable to finite plastic deformation collisions. Li et al. [16] assumed a relationship between the contact radius and the maximum pressure at the contact centre, improved the model of Johnson [17], and obtained a theoretical model for the coefficient of restitution at low velocities. Jackson and Green used a finite element method to simulate the contact between an elastoplastic hemisphere and a rigid plane. They proposed an empirical formula for the contact area based on material properties and collision depth in 2005 [18]. The well-known JGM model was proposed by Robert L. Jackson, Itzhak Green and Dan B. Marghitu. Two sets of empirical equations for the coefficient of restitution were obtained because they used different residual perturbation equations to derive the recovery phase. During their analysis, they found the expression for the critical velocity that leads to plastic deformation of the impacting sphere [19]. Daolin Ma and Caishan Liu used the continuity of contact force and collision depth, as well as the geometric relationship during the collision, to derive the relationship between force and collision depth, which led to the expression of the coefficient of restitution [20]. Deepak Patil and C. Fred Higgs III studied the nonlinear relationship between the ratio of plate thickness to sphere diameter. They obtained a critical plate thickness of twice the diameter of the sphere, below which the effect of bending vibration becomes apparent. The coefficient of restitution cannot be considered a constant, and when the plate thickness is greater than the critical thickness, the error in using a constant coefficient of restitution is less [21]. Wang et al. proposed a contact force model with a variable coefficient of restitution [22]. Liu et al. improved and optimised the JGM model by introducing the yield strength into the JGM model [23]. Itzhak Green combined the JGM model with the Zener model to form a coefficient of restitution model that considers the effects of both plastic deformation and elastic waves [24].

Several studies have now demonstrated that there is a link between the modulus of elasticity and the thickness of the collision, and the relationship is shown in Figure 1 for certain plate thickness ranges. However, this factor has not been taken into account in existing models.

This paper proposes a plate thickness influence factor with the ratio of sphere diameter to plate thickness as a variable. The plate thickness influence factor optimises the widely accepted JGM model, and a new coefficient of restitution model is obtained, which can consider the finite plate thickness. The new model is then compared and analysed with other models, and the results show that the new model works well. Finally, the model's validity has been verified using data, which shows that the model can predict the coefficient of restitution for a specific plate thickness range.

2 The JGM Model

The JGM model [19] is the classical coefficient of restitution model and has been shown in Ref. [23] to be well-suited to materials with different yield strengths. Therefore, this paper uses the JGM model for improvement and optimization. A schematic diagram of the contact model used for the JGM model is shown in Figure 2. The model analyses three main stages in the collision process. The analysis process is as follows.

The equivalent modulus of the contact body is:

$$E' = \frac{E'_a E'_b}{E'_a + E'_b}, \tag{1}$$

$$E'_i = \frac{E_i}{1 - v_i^2}, \quad i = a, b, \tag{2}$$

where v is the Poisson's ratio, and a, b represent the two contact bodies, respectively.

In 2005, Jackson and Green [18] obtained an expression for the critical collision depth leading to plastic deformation of an impacting sphere as a function of yield strength

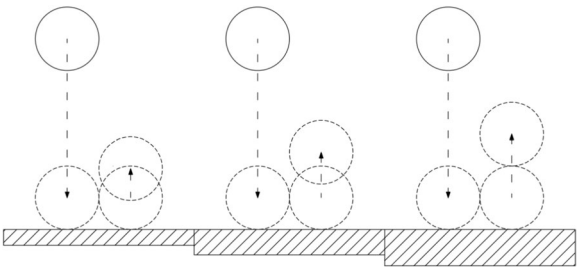

Figure 1 Schematic representation of the relationship between the coefficient of restitution and collision thickness

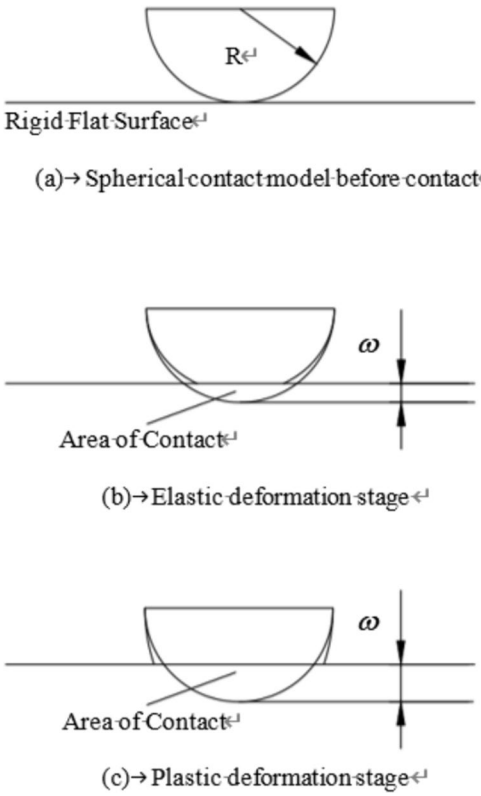

Figure 2 Spherical contact model schematic

$$\omega_c = \left(\frac{\pi C S_y}{2E'}\right)^2 R, \tag{3}$$

$$C = 1.295e^{0.736\nu}, \tag{4}$$

$$\frac{1}{R} = \frac{1}{R_a} + \frac{1}{R_b}, \tag{5}$$

where R is the equivalent radius of contact, and S_y is the yield strength. To use the Poisson's ratio and yield strength values of the first material to yield in Eq. (4), C and S_y can be considered in combination. In taking the value, the parameter is taken to be the minimum of this parameter for both materials

$$CS_y = \min\left(C(\nu_a)S_{ya}, C(\nu_b)S_{yb}\right). \tag{6}$$

2.1 Elastic Compression Phase

After the start of the collision, before reaching the critical collision depth, the collision process mainly occurs in elastic deformation. When conducting an analysis of energy conservation within the collision process, the following can be derived:

$$\frac{1}{2}mv^2 - \frac{1}{2}m(V_1)^2 = -\int_0^{\omega}(P_e)\mathrm{d}x, \tag{7}$$

where v is the instantaneous velocity during the collision, V_1 is the initial velocity before the collision, m is the mass of the ball, P_e and x are the contact forces and dummy variables corresponding to the instantaneous velocity during the collision, and ω is the collision depth during the collision. Substituting the Hertz contact force represented by Eq. (8) into Eq. (7), we get:

$$P = \frac{4}{3}E'\sqrt{R}x^{\frac{3}{2}}, \tag{8}$$

$$\frac{1}{2}mv^2 - \frac{1}{2}m(V_1)^2 = -\frac{8}{15}E'\sqrt{R}\omega^{5/2}. \tag{9}$$

From Eqs. (8) and (9), we can obtain the instantaneous velocity during the collision as follows:

$$v = \sqrt{V_1^2 - \frac{16}{15}\frac{E'}{m}\sqrt{R}\omega^{5/2}}. \tag{10}$$

The elastic deformation phase ends when the critical collision depth is reached, at which point the instantaneous velocity is:

$$v_c = \sqrt{V_1^2 - \frac{16}{15}\frac{E'}{m}\sqrt{R}\omega_c^{5/2}}. \tag{11}$$

2.2 Elastoplastic Compression Phase

After the critical collision depth is reached, the collision process enters the elastoplastic phase. From the derivation of the elastic compression phase, it can be seen that the kinetic energy lost in the elastic compression phase is:

$$\Delta W_{\mathrm{e}} = \frac{8}{15}E'\sqrt{R}\omega_c^{5/2}. \tag{12}$$

Then, applying the law of conservation of energy during elastoplastic compression, we get:

$$\frac{1}{2}mv^2 - \frac{1}{2}m(V_1)^2 = W_{ep} - \Delta W_e, \tag{13}$$

where W_{ep} is the kinetic energy loss during elastoplastic deformation can be expressed as:

$$W_{ep} = -\int_{\omega_c}^{\omega}(P_{ep})\mathrm{d}x, \tag{14}$$

where P_{ep} is the contact force in the elastoplastic phase. When the compression process reaches its maximum, the instantaneous velocity of the collision decreases to 0, at which point the collision depth displacement caused by the collision reaches its maximum. From Eqs. (12) (13) (14), we can obtain:

$$-\frac{1}{2}m(V_1)^2 = -\int_{\omega_c}^{\omega_m}\left(P_{ep}\right)\mathrm{d}x - \frac{8}{15}E'\sqrt{R}\omega_c^{5/2}, \quad (15)$$

where ω_m is maximum depth during collision.

2.3 Restitution Phase

When the collision depth reaches its maximum, the compression phase of the collision process has been completed, and the contact force has reached its maximum. The collision then enters the restitution phase. Under perfectly elastic conditions, the sphere can return to its state at the start of the collision. However, if the elastoplastic phase of the collision process occurs, the sphere will not be able to return to its original shape. Assuming that the radius of curvature becomes R_{res} and that the surface has a residual collision depth,ω_{res}, the maximum contact force $\left(P_{ep}\right)_m$ during the recovery process can be expressed as

$$\left(P_{ep}\right)_m = \frac{4}{3}E'\sqrt{R_{res}}(\omega_m - \omega_{res})^{3/2}. \quad (16)$$

Two methods are used in the JGM model to obtain the radius of curvature,R_{res}, and the residual collision depth, ω_{res}. The first is the method of Etsion [25].

$$\frac{\omega_{res}}{\omega_m} = 1 - \frac{3(P_{ep})_m}{4E'a_m\omega_m}, \quad (17)$$

$$R_{res} = \frac{4E'(a_m)^3}{3(P_{ep})_m}, \quad (18)$$

where a_m is the contact radius at which the maximum contact force is achieved.

The second method is the result of Jackson in 2005 using the finite element approach [26].

$$\frac{\omega_{res}}{\omega_m} = 1.02\left(1 - \left(\frac{\frac{\omega_m}{\omega_c} + 5.9}{6.9}\right)^{-0.54}\right), \quad (19)$$

$$R_{res} = \frac{1}{(\omega_m - \omega_{res})^3}\left(\frac{4(P_{ep})_m}{3E'}\right)^2. \quad (20)$$

At the end of the restitution phase, the sphere will be out of contact with the plane, at which point the velocity of the sphere can be solved for by Eq. (21).

$$\frac{1}{2}m(V_2)^2 = \int_{\omega_m-\omega_{res}}^{0}\left(\frac{4}{3}E'\sqrt{R_{res}}(x)^{3/2}\right)\mathrm{d}x. \quad (21)$$

By solving and simplifying Eq. (21), we obtain:

$$V_2 = \sqrt{\frac{16E'}{15m}}(R_{res})^{1/4}(\omega_m - \omega_{res})^{5/4}. \quad (22)$$

Jackson analyzed the restitution phase of the collision process using each of the two methods mentioned above and summarized the empirical formulae for the two coefficient of restitution prediction models.

The empirical formula I:

$$\begin{cases} e = 1, & 0 < V_1^* \le 1, \\ e = 1 - 0.1\ln\left(V_1^*\right)\left(\frac{V_1^*-1}{59}\right)^{0.156}, & 1 < V_1^* \le 60, \\ e = 1 - 0.1\ln(60) - 0.11\ln\left(\frac{V_1^*}{60}\right)\left(V_1^* - 60\right)^{2.36\varepsilon_y}, & 60 < V_1^* \le 1000. \end{cases} \quad (23)$$

The empirical formula II:

$$\begin{cases} e = 1, & 0 < V_1^* \le 1, \\ e = 1 - 0.0361\left(\varepsilon_y\right)^{-0.114}\ln\left(V_1^*\right)\left(V_1^* - 1\right)^{9.5\varepsilon_y}, & V_1^* > 1, \end{cases} \quad (24)$$

where $V_1^* = \frac{V_1}{V_c}$, $\varepsilon_y = \frac{S_y}{E'}$.

3 Acquisition of Plate Thickness Influence Factor

The JGM model is obtained by analyzing the collision process between a sphere and a rigid plane. Therefore, the influence of the actual plate thickness on the coefficient of restitution is not considered. However, the objects colliding are often not rigid, and therefore, the plate thickness may significantly affect the coefficient of restitution. Ref. [21] shows that when the plate thickness is less than twice the sphere's diameter, the coefficient of restitution varies with the plate thickness. Otherwise, the coefficient of restitution of the sphere does not vary with plate thickness. Instead, it is closer to a constant.

Based on the conclusions of Ref. [19], the JGM model effectively predicts the coefficient of restitution when the plate thickness is more significant than twice the diameter of the sphere. Therefore, under this condition, the prediction result of the optimized JGM model should be close to that of the JGM model. On the other hand, when the plate thickness is less than twice the sphere diameter,

the JGM model will produce a more significant deviation. The plate thickness impact factor is considered to be added to the JGM model to allow better prediction of the coefficient of restitution for plate thicknesses less than twice the sphere diameter and similar results to the JGM model for plate thicknesses greater than twice the sphere diameter.

$$e = \lambda e_{JGM}, \tag{25}$$

where e_{JGM} is the coefficient of restitution derived from the JGM model and λ is the plate thickness influence factor.

The Zener model considers the effect of plate thickness but only considers energy loss in the form of bending vibrations. As a result, the coefficient of restitution is well predicted in the case of thin plates; if the plate thickness is too large, plastic deformation becomes the dominant form of energy loss, and the coefficient of restitution becomes inaccurate.

Since the Zener model considers the effect of plate thickness, we can refer to the Zener model to generate a plate thickness influence factor. In the Zener model, the coefficient of restitution is a function of the square of the ratio of the sphere diameter to the plate thickness [21]. Accordingly, the plate thickness influence factor λ can be assumed to be

$$\lambda = k_1\left(\frac{d}{t}\right)^2 + k_2\left(\frac{d}{t}\right) + k_3. \tag{26}$$

For the above equation, it is necessary to select the best parameter k_1 k_2 k_3 to form the optimal plate thickness influence factor λ. The corresponding parameter k_1 k_2 k_3 can be obtained by fitting experimental data from Ref. [21].

The experimental data in Ref. [21] were obtained by varying plate thickness, sphere diameter, and material at three different impact velocities. The ratio of sphere diameter to plate thickness is an essential variable in investigating the relationship between plate thickness and the coefficient of restitution. Therefore, the case at one velocity can be used as a basis for fitting the λ and using Eq. (26) to obtain the variables $k_1k_2k_3$ in the plate thickness influence factor. The fitting process involves finding the ratio of the experimental coefficient of restitution to the predicted result of the JGM model, which is also the plate thickness influence factor λ. The results of the fitting are shown in Figure 3. The property parameters of the experimental materials are given in Table 2, where borosilicate glass is a brittle material. Its yielding was not considered during the collision, so the experimental data

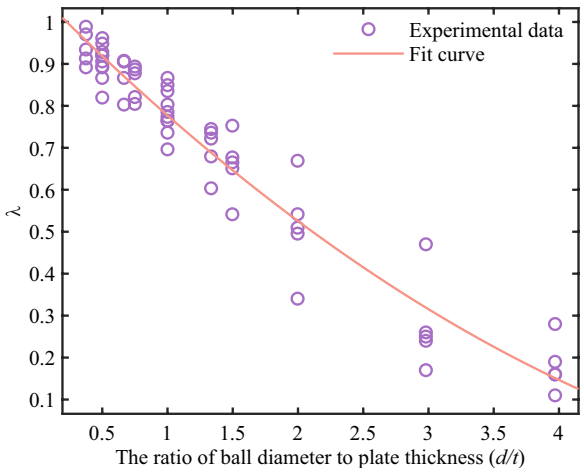

Figure 3 Fitting curves of COR values for various materials for impact velocity V_1 = 1.1 m/s [21]

where the sphere material was borosilicate glass was not analyzed in the subsequent process.

The fit results are expressed as Eq. (27).

$$\lambda = 0.02077\left(\frac{d}{t}\right)^2 - 0.314\left(\frac{d}{t}\right) + 1.07. \tag{27}$$

The fitting results in Figure 3 show that there is indeed a particular pattern in the distribution of the experimental data, which is roughly distributed around a specific curve. Therefore, an improved approach to the JGM model using the plate thickness influence factor is feasible. It is also observed that when the plate thickness is greater than twice the sphere diameter, the distribution of the coefficient of restitution becomes progressively more concentrated as the ratio of sphere diameter to plate thickness decreases. That proves the existence of the critical plate thickness proposed in Ref. [21].

The experimental coefficient of restitution has an increasing data dispersion as the ball diameter-to-plate thickness ratio increases. As the ball diameter to plate thickness ratio increases, the plate becomes thinner and the primary form of energy dissipation during collision shifts from plastic deformation to bending vibration. At this point, the coefficient of restitution becomes closer to that predicted by the Zener model. Therefore, It is understandable that the fitted curve becomes less effective as the ratio of sphere diameter to plate thickness increases.

The experimental data for the coefficient of restitution for a sphere material of brass alloy 260 and a plate of aluminum 6061 at an initial collision velocity of 1.1 m/s are given in Table 1 as an example. As shown in Case 1 in

Table 1 COR value of brass alloy for impact velocity *V*= 1.1 m/s [21]

d/t	COR (JGM)	COR (experimental)	Case 1			Case 2		
			λ	COR (improved)	Error %	λ	COR (improved)	Error %
3.969	0.738	0.120	0.151	0.111	7.110	–	–	–
2.975	0.738	0.190	0.320	0.236	24.235	–	–	–
1.997	0.738	0.400	0.526	0.388	2.937	0.526	0.388	2.973
1.497	0.738	0.500	0.647	0.477	4.522	0.663	0.490	2.092
1.334	0.738	0.550	0.688	0.508	7.624	0.706	0.521	5.241
1.000	0.738	0.580	0.777	0.574	1.110	0.791	0.584	0.680
1.000	0.738	0.640	0.777	0.574	10.381	0.791	0.584	8.759
0.750	0.738	0.660	0.846	0.625	5.319	0.852	0.629	4.681
0.666	0.738	0.670	0.870	0.642	4.119	0.872	0.644	3.915
0.500	0.738	0.710	0.918	0.678	4.509	0.911	0.673	5.280
0.499	0.738	0.660	0.918	0.678	2.742	0.911	0.673	1.910
0.375	0.738	0.730	0.955	0.705	3.379	0.939	0.694	4.975

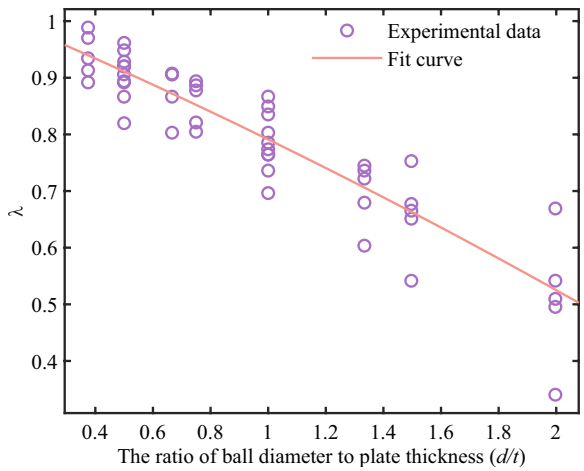

Figure 4 Fitting curves of COR values for various materials for impact velocity Vi = 1.1 m/s (d/t<2) [21]

Table 1, the predicted coefficient of restitution appears to be more inaccurate for sphere diameters greater than twice the plate thickness than for the other cases. The same situation occurs with experimental data for different sphere materials, indicating that the new model for predicting the coefficient of restitution becomes less applicable in this range of plate thicknesses.

When the ratio of ball diameter to plate thickness is large, the form of energy loss at this time is dominated by bending vibration. This is inconsistent with the assumptions of the JGM model. Therefore, we can choose a relatively small range of the ratio of ball diameter to plate thickness to improve the JMG model.

To ensure that the new model has a good prediction of the coefficient of restitution within a reasonable range. The data with significant errors, the ratio of sphere diameter to plate thickness greater than 2, were eliminated before fitting the curve. The new results of the fit are shown in Figure 4 and Case 2 in Table 1.

The fitting result is expressed in the form of Eq. (26):

$$\lambda = -0.01747\left(\frac{d}{t}\right)^2 - 0.2137\left(\frac{d}{t}\right) + 1.022, \quad 0 < \frac{d}{t} < 2. \tag{28}$$

Experimental data with a sphere material of brass alloy 260 and an initial collision velocity of 1.1 m/s are used as an example. For the ratio of sphere diameter to plate thickness less than 2, the predicted coefficient of restitution did not show a significant increase in error within a specific range. When the sphere diameter to plate thickness ratio is less than 0.5, the plate thickness influence factor reaches more than 0.9. At this point, the critical plate thickness has been reached. That is, the plate thickness is greater than twice the sphere diameter, and in this range, the coefficient of restitution does not change with the change in the ratio of sphere diameter to plate thickness but is closer to a constant. Suppose the ball diameter to plate thickness ratio is infinitesimally small, which means it is close to zero. In that case, the coefficient of restitution is 1.022 times the value of the JGM model. This error is acceptable.

By combining Eqs. (25) and (28), we can obtain a new model for predicting the coefficient of restitution:

$$e = \left(-0.01747\left(\frac{d}{t}\right)^2 - 0.2137\left(\frac{d}{t}\right) + 1.022\right)e_{JGM}, \quad 0 < \frac{d}{t} < 2. \tag{29}$$

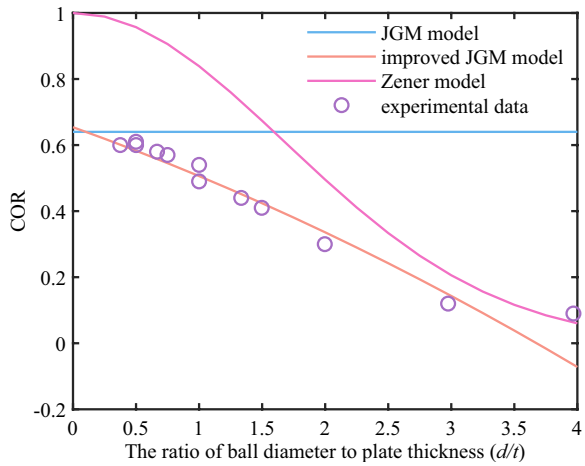

Figure 5 Comparison between different models

To verify that the improved coefficient of restitution prediction model has better prediction results, we need to compare the new model with other models for analysis.

Data from experimental conditions where the sphere material is low carbon steel and the initial collision velocity is 2.3 m/s are used as examples. The trends of the JGM model, the Zener model, and the improved JGM model are compared and analyzed for different ratios of sphere diameter to plate thickness, and the comparison is shown in Figure 5. According to Ref. [21], the Zener model is calculated as

$$e_{Zener} = \exp\left(-1.7191\eta\right), \tag{30}$$

$$\eta = \frac{1}{4\sqrt{3}}\left(\frac{\pi\rho_a}{\rho_b}\right)^{3/5}\left(\frac{d}{t}\right)^2\left(\frac{V_1^2\rho_b}{E_b'}\right)^{1/10}\left(1+\frac{E_b'}{E_a'}\right)^{-2/5}, \tag{31}$$

where ρ_a and ρ_b are the densities of the sphere and plate, respectively.

A comparison of the plots (Figure 5) shows that the Zener model effectively predicts the coefficient of restitution when the ratio of sphere diameter to plate thickness is significant when the plate thickness is relatively small. Both the JGM model and the improved JGM model can predict the coefficient of restitution more accurately when the ratio of sphere diameter to plate thickness is large. However, when the sphere diameter to plate thickness ratio is 0.5 to 2, the improved JGM model has better prediction results, proving that the plate thickness influence factor λ can optimize and improve the JGM model.

Experimental data under different experimental conditions will validate the improved JGM model in the next chapter.

4 Verification

Further validation and analysis of the above model can be carried out using experimental data on the coefficient of restitution at other initial collision speeds. The parameters of the materials used for the experiments are given in the following tables. Table 2 shows the main property parameters for the sphere and plate materials.

Table 2 shows the main parameters used in the JGM and Zener models to calculate the coefficient of restitution. The yield strength of the brittle material is unknown in Table 2, indicating that the brittle material does not yield during the collision.

From the above analysis, it can be seen that the obtained improved JGM model is applicable in the range of $0 \le d/t \le 2$, outside of which the prediction error for the coefficient of restitution becomes large. Therefore, the coefficient of restitution of different sphere materials with the ratio of sphere diameter to plate thickness below two was chosen to validate the improved JGM model.

Experimental data with an initial collision velocity of 1.1 m/s were used to fit the plate thickness influence factor. Since the JGM model can predict the coefficient of restitution of an object at different initial collision velocities, whether the method of using plate thickness influence factors is reasonable and accurate can be verified by the coefficients of restitution of the objects at different initial collision velocities. A comparison of the simulation results of the improved coefficient of restitution model with the actual experimental results under different

Table 2 Material properties

Material	Geometry	Elastic Modulus (GPa)	Poisson's Ratio	Yield Strength (GPa)	Density (kg/mm^3)
Brass Alloy 260	Sphere	103	0.35	0.393	8525
Aluminium 1100-H16	Sphere	70	0.33	0.103	2710
Tungsten Carbide	Sphere	621	0.18	1.720	14950
S2 Tool Steel	Sphere	207	0.30	2.00	7861
Low Carbon Steel	Sphere	200	0.30	0.303	7833
Aluminium 6061	Plate	69	0.33	0.290	2700

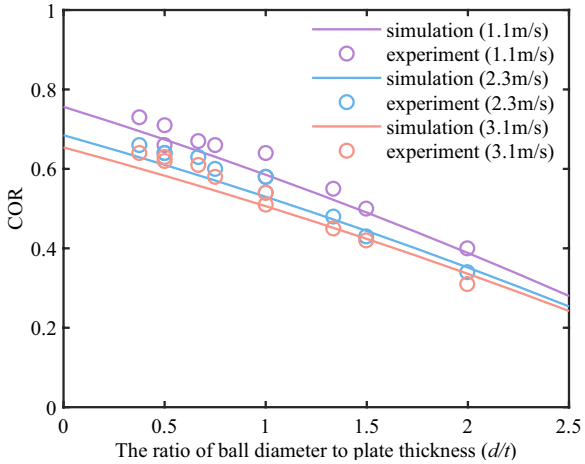

Figure 6 Comparison of experimental and simulated COR results for brass alloy spheres [21]

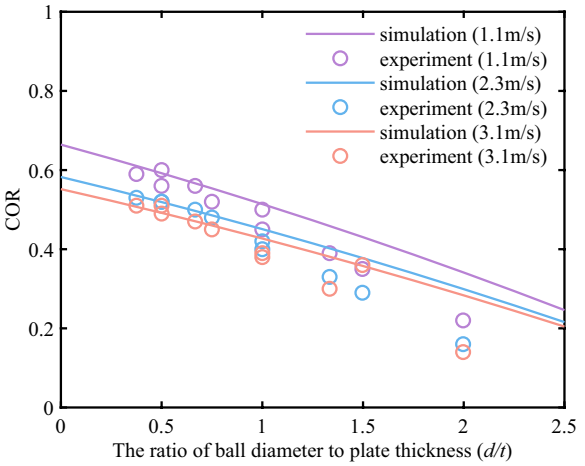

Figure 8 Comparison of experimental and simulated COR results for tungsten carbide [21]

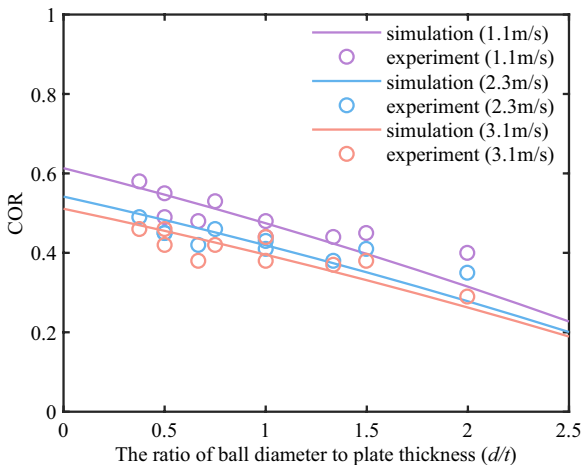

Figure 7 Comparison of experimental and simulated COR results for aluminum 1100-H16 [21]

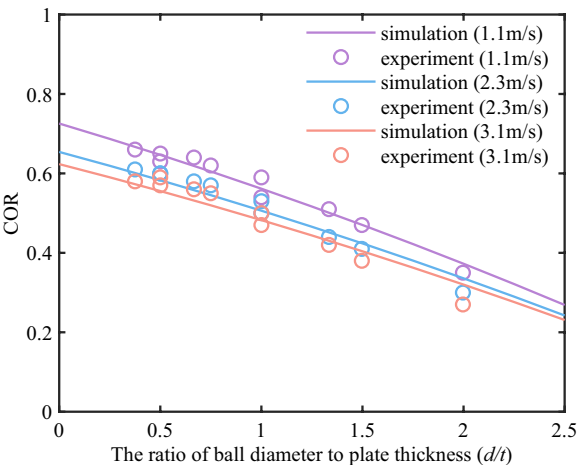

Figure 9 Comparison of experimental and simulated COR results for S2 tool steel [21]

conditions is shown in Figures 6, 7, 8, 9, and 10. The data in the figure are taken from Ref. [21].

By comparison, we can see that the improved JGM model has a better prediction of the coefficient of restitution in the range of spheres made of brass alloy spheres, aluminum 1100-H16, S2 tool steel, and low carbon steel. Furthermore, this prediction is not degraded by changing the initial collision velocity.

In the comparison plots where the sphere material is tungsten carbide, a relatively large error occurs when d/t is approximately 2. That may be due to roughness and needs to be investigated further. Nevertheless, the improved JGM model can still accurately predict the coefficient of restitution within the $0 \leq d/t \leq 1.5$ range.

To ensure the conclusions' reliability, we conducted experiments to determine the coefficient of restitution for impacts between S2 tool steel and 6061 aluminum. Figure 11 shows the experimental setup.

The experimental setup controls the initial collision velocity when an impact occurs by controlling the height of the distance between the ball and the plate. The data collector receives and stores the signal generated by the acceleration sensor.

$$\dot{\delta}^{-} = \sqrt{2g(H-R)}, \tag{32}$$

where g represents the acceleration due to gravity, H represents the initial height of the ball's center of mass from

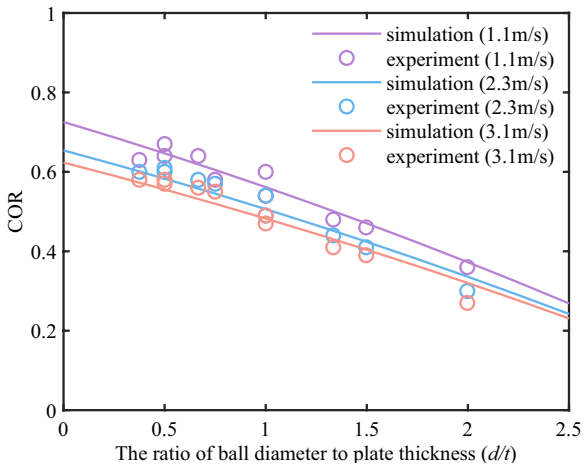

Figure 10 Comparison of experimental and simulated COR results for low-carbon steel [21]

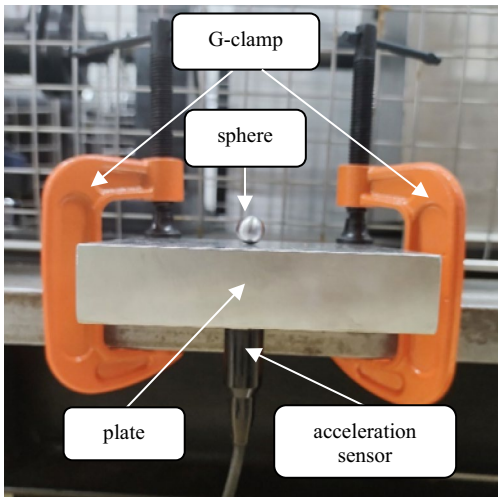

Figure 11 Drop test apparatus

the ground, and R represents the radius of the ball. $\dot{\delta}^-$ represents the impact velocity.

Table 3 displays the relevant parameters of the experiments. Five experiments were conducted, with plate thicknesses of 6 mm, 10 mm, 14 mm, 18 mm, and 22 mm.

After the impact with the plate, the sphere will rebound and continue to fall, resulting in a second impact between the sphere and the plate. Experimental data can be used to determine the time interval between the first impact and the second impact. Assuming the resistance of the sphere is not a factor during the rebound process, we can calculate the velocity after a collision using Eq. (33).

$$\dot{\delta}^+ = -\mathrm{g}\frac{(t_2-t_1)}{2}, \tag{33}$$

where, t_1 and t_2 represent the time of the first and second impact, respectively, and $\dot{\delta}^+$ represents the separation speed. The coefficient of restitution for the first impact process can be calculated using Eqs. (32) and (33). Table 4 displays the data obtained and analyzed during the experiment.

The plate thickness of 6 mm is used as an example to illustrate the acquisition of post-collision velocity. In Figure 12, the horizontal coordinate of the first peak is the time of the first collision, t_1, and the horizontal coordinate of the second peak is the time of the second collision, t_2. After that, the post-collision velocity can be obtained by using Eq. (33).

The coefficient of restitution obtained from the experiments generally agrees with the coefficient of restitution predicted by the improved JGM model. Comparing the coefficient of restitution obtained experimentally with the coefficient of restitution predicted by the model, we placed both of them in a graph and presented the results in Figure 13.

5 Conclusions

Existing models are ineffective in predicting the coefficient of restitution in the case of finite plate thickness. This paper proposes a generalized equation for the plate thickness influence factor concerning the Zener model applicable to thin plate collisions to address this shortcoming. The specific expression of the plate thickness influence factor is then determined from experimental data, and the JGM model is optimized using the plate thickness influence factor. The improved JGM model was compared and analyzed with the JGM and Zener models. The results show that the new model has a better prediction ability for limited plate thickness.

Table 3 Relevant parameters of the test material

Material	Geometry	Elastic Modulus (GPa)	Poisson's Ratio	Yield Strength (GPa)	Density (kg/mm^3)	Size
S2 Tool Steel	Sphere	207	0.30	2.00	7861	d=10mm
Aluminum 6061	Plate	69	0.33	0.29	2700	t=6mm, 10mm, 14mm, 18mm, 22mm

Table 4 Experimental data and analysis

Plate Thickness (mm)	*d*/*t*	COR (theoretical)	t_2-t_1 (s)	Impact Velocity (m/s)	Separating Velocity (m/s)	COR (experimental)	Error (%)
6	1.67	0.43	0.0959	1.1287	0.4699	0.42	3.65
10	1.00	0.55	0.1313	1.1287	0.6434	0.57	2.97
14	0.71	0.60	0.1360	1.1287	0.6664	0.59	1.98
18	0.56	0.63	0.1476	1.1287	0.7232	0.64	1.95
22	0.45	0.64	0.1504	1.1287	0.7370	0.65	1.25

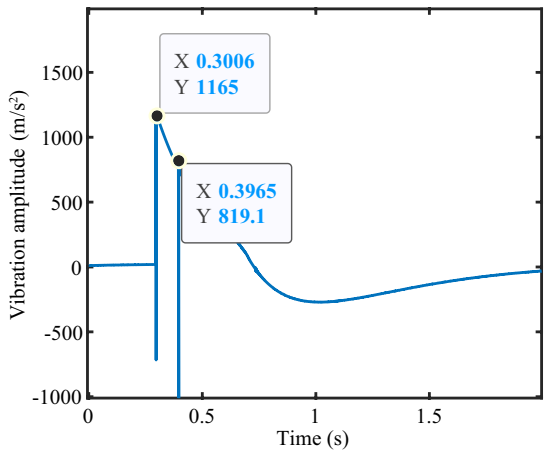

Figure 12 Collision process for a plate thickness of 6mm

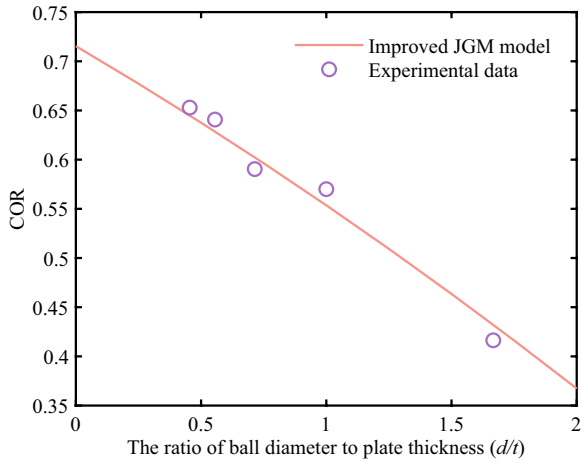

Figure 13 Comparison of the results for the coefficient of restitution

After that, the improved model was validated using data at different collision velocities. The results show that the model predictions agree with the experimental results. Finally, sphere-plate collision experiments with varying thicknesses of the plate were conducted to make the conclusions more reliable. The results indicate that almost all data are close to the model simulation results within a specific plate thickness range, confirming the new model's validity and reasonableness.

The improved model overcomes the limitations of its predecessor, which could not precisely predict the coefficient of restitution with a finite thickness. In addition, this model provides the theoretical basis for analyzing the impacting process and the contacting force. It also aids in the diagnosis and analysis of rub-impact failure.

Acknowledgements
Not applicable.

Author Contributions
YF was in charge of the whole trial and wrote the manuscript; HW provided many suggestions on the research background. TZ assisted with sampling and laboratory analyses; MH provided lab and writing instructions; LZ and ZJ gave a lot of advice on thesis writing. All authors read and approved the final manuscript.

Funding
Supported by Joint Fund of the Ministry of Education of China (Grant No. 8091B022203), Youth Talent Support Project (Grant No. 2022-JCJQ-QT-059).

Data availability
Data will be made available on request.

Declarations

Competing Interests
The authors declare no competing financial interests.

Received: 13 January 2024 Revised: 26 June 2024 Accepted: 1 July 2024
Published online: 19 August 2024

References

[1] Xiaofeng Liu, Chi Zhang, Lin Bo, et al. Effects of cross stiffness on dynamic characteristics of rubbing rotor. *Journal of Vibration and Shock*, 2021,40(11): 176-181, 219.
[2] Zhou Tao, Minghui HU, Ya HE, et al. Vibration features of rotor unbalance and rub-impact compound fault. *Journal of Advanced Manufacturing Science and Technology*, 2022, 2(1): 2022002. 10.51393/j. jamst. 2022002
[3] Feiyun Cong, Jin Chen, Guangming Dong, et al. Experimental validation of impact energy model for the rub–impact assessment in a rotor system. *Mechanical Systems and Signal Processing*, 2011, 25(7): 2549-2558.
[4] Pingchao Yu, Cun Wang, Hou Li, et al. Dynamic characteristics of an aero-engine dual-rotor system with inter-shaft rub-impact. *Mechanical Systems and Signal Processing*, 2022, 166: 108475.

[5] Xiantao Zhang, Yongfeng Yang, Hui Ma, et al. A novel diagnosis indicator for rub-impact of rotor system via energy method. *Mechanical Systems and Signal Processing*, 2023, 185: 109825.
[6] Yu Li, Caifeng Wang, Chao Jiang, et al. Analysis on dynamic characteristics of coupling misalignment-rotor system's windmill rub coupled fault. *Journal of Machine Design*, 2022, 39(12): 101-110. (in Chinese)
[7] Newton I. *Philosophiae naturalis principia mathematica*. Apud.Guil.&Joh. Innys,1726
[8] K H Hunt, F R Crossley, Coefficient of restitution interpreted as damping in vibroimpact. *Journal of Applied Mechanics*, 1975, 42(2):440.
[9] C W Kilmister, J E Reeve. *Rational mechanics*. Upper Saddle River, NJ: Prentice Hall Press,1966
[10] W J Stronge. Rigid body collisions with friction. *Proceedings of Royal Society of London,* 1990, A431: 169–181.
[11] W J Stronge. *Impact Mechanics*. Cambridge: Cambridge University Press, 2000.
[12] Paulo Flores, Margarida Machado, Miguel T. Silva, et al. On the continuous contact force models for soft materials in multibody dynamics. *Multibody System Dynamics*, 2011, 25: 357–375.
[13] W L Yao, R Yue. Advance in controversial restitution coefficient study for impact problem. *Journal of Vibration and Shock*, 2015, 34(19): 43-48 (in Chinese).
[14] C Thorton. Coefficient of restitution for collinear collisions of elastic-perfectly plastic spheres. *Journal of Applied Mechanics*, 1997, 64(2): 383-386.
[15] C Y Wu, L Y Li, C Thornton. Energy dissipation during normal impact of elastic and elastic–plastic spheres. *International Journal of Impact Engineering*, 2005, 32(1/4): 593-604.
[16] L Y Li, C Y Wu, C Thornton. A theoretical model for the contact of elastoplastic bodies. *Proceedings of the Institution of Mechanical Engineers, Part C: Journal of Mechanical Engineering Science,* 2001, 216(4): 421-431.
[17] K L Johnson. *Contact mechanics*. American Society of Mechanical Engineers, 1985.
[18] R L Jackson, I Green. A finite element study of elasto-plastic hemispherical contact against a rigid flat. *ASME. J. Tribol*., 2005, 127(2): 343–354.
[19] R L Jackson, Green I, B Dan, et al. Predicting the coefficient of restitution of impacting elastic-perfectly plastic spheres. *Nonlinear Dynamics*, 2010, 60(3): 217-229.
[20] Daolin Ma, Caishan Liu. Contact law and coefficient of restitution in elastoplastic spheres. *Journal of Applied Mechanics*, 2015, 82(12): 121006.
[21] Deepak Patil, C. Fred Higgs III. Experimental investigations on the coefficient of restitution for sphere-thin plate elastoplastic impact. *Journal of Tribology*, 2018, 140(1): 011406.
[22] Xupeng Wang, Yan Zhang, Xiaomin Ji, et al. A contact-impact force model based on variable recovery coefficient. *Journal of Vibration and Shock*, 2019, 38(5): 198-202. (in Chinese).
[23] Xichun Liu, Wei Chen, Hu Shi. Improvement of contact force calculation model considering influence of yield strength on coefficient of restitution. *Energies*, 2022, 15(3): 1041.
[24] I Green. The prediction of the coefficient of restitution between impacting spheres and finite thickness plates undergoing elastoplastic deformations and wave propagation. *Nonlinear Dyn.,* 2022, 109(4): 2443–2458.
[25] I Etsion, Y Kligerman, Y Kadin. Unloading of an elastic–plastic loaded spherical contact. *International Journal of Solids and Structures*, 2005, 42(13): 3716-3729.
[26] R Jackson, I Chusoipin, I Green. A finite element study of the residual stress and deformation in hemispherical contacts. *ASME. Journal of Tribology*, 2005, 127(3): 484-493.

Yunfeng Fan born in 1998, is currently a master's degree candidate at *College of Mechanical and Electrical Engineering, Beijing University of Chemical Technology, China*.

Hao Wang born in 1992, is currently an engineer at *China Ship Research and Development Academy, China.*

Tao Zhou born in 1999, is currently a master's degree candidate at *College of Mechanical and Electrical Engineering, Beijing University of Chemical Technology, China.*

Limin Zou born in 1960, is currently a professor at *College of Mechanical and Electrical Engineering, Beijing University of Chemical Technology, China*.

Zhinong Jiang born in 1967, is currently a researcher at *College of Mechanical and Electrical Engineering, Beijing University of Chemical Technology, China.* His main research interests are condition monitoring and fault diagnosis.

Minghui Hu born in 1990, is currently a professor at *College of Mechanical and Electrical Engineering, Beijing University of Chemical Technology, China*. His main research interests are fault diagnosis and vibration suppression of aero-engine.